N^1-(5′-Phosphoribosyl)adenosine−5′-Monophosphate Cyclohydrolase: Purification and Characterization of a Unique Metalloenzyme†

Robert L. D'Ordine, Thomas J. Klem,‡ and V. Jo Davisson*

Department of Medicinal Chemistry and Molecular Pharmacology, 1333 Robert Heine Pharmacy Building, Purdue University, West Lafayette, Indiana 47907-1333

Received October 16, 1998; Revised Manuscript Received December 7, 1998

ABSTRACT: N^1-(5′-Phosphoribosyl)adenosine−5′-monophosphate cyclohydrolase (HisI, PR-AMP cyclohydrolase) is a central enzyme in histidine biosynthesis catalyzing the hydrolysis of the N1−C6 bond of the purine substrate, a reaction unique to this pathway. A source of the recombinant monofunctional *Methanococcus vannielii* PR-AMP cyclohydrolase has been developed, and the first characterization of a purified form of the enzyme is reported. The enzyme has a native molecular weight of 31 200 as determined by analytical ultracentrifugation that agrees with the molecular mass determined by gel filtration (34 kDa) and a subunit molecular weight of 15 486 based on MALDI-MS. An unusual characteristic of the protein is the complexity observed on SDS−PAGE, and N-terminal amino acid sequence analysis of all the isolated constituents confirms their origin as PR-AMP cyclohydrolase. A highly conserved region of the amino acid sequence is implicated in the self-cleavage events of the protein and provides an explanation for the complexity of this protein. Bound to the enzyme is 1 equiv of Zn^{2+} that can be removed only by extended dialysis with 1,10-phenanthroline ($K_d \leq 10^{-9}$ M). Removal of the Zn^{2+} correlates with the loss of enzyme activity. The enzyme is reversibly inhibited by inclusion of EDTA in the assay mixture, demonstrating that free Mg^{2+} ($K_s = 4.9 \pm 0.7$ μM) is required for catalytic activity. Further evidence for a low-affinity binding site is indicated by the inhibitory effects of exogenous Zn^{2+} on enzyme activity. The pH dependence of the PR-AMP cyclohydrolase activity shows a single titration event in the k_{cat}/K_m profile with a pK_a of 7.3 that is consistent with the functional role of a metal site in catalysis. These data are discussed in the context of the mechanism of other nucleotide hydrolases.

The de novo biosynthesis of histidine occurs in plants and microorganisms and maintains an integrated role in the balance of cellular nitrogen metabolism (*1*, *2*). Histidine production is accomplished at significant metabolic expense, highlighted by the precursors ATP and 5-phospho-D-ribosyl-1-pyrophosphate (PRPP[1]), and requires integration with de novo purine metabolism. Partial catabolism of a purine nucleus to recycle carbon and nitrogen for the production of another essential metabolite occurs only in the case of histidine, although related processes are involved in production of the vitamins folic acid, riboflavin, and thiamin (*3*, *4*). A key step for utilizing the purine heterocycle of ATP in histidine biosynthesis involves hydrolytic cleavage of the unusual nucleotide N^1-(5′-phosphoribosyl)adenosine 5′-monophosphate (PR-AMP). The enzyme that catalyzes this reaction is the focus of this paper.

PR-AMP cyclohydrolase catalyzes the hydrolysis of the adenine ring of N^1-(5′-phosphoribosyl)adenosine 5′-monophosphate (PR-AMP) between N1 and C6 (Scheme 1). Smith and Ames originally described the enzyme activity (*5*), but a detailed characterization has not been conducted prior to this study. The preceding step in the pathway involves the hydrolytic removal of pyrophosphate from N^1-(5′-phosphoribosyl)adenosine triphosphate (PR-ATP) catalyzed by HisE and represents the commitment of the nucleotide to histidine biosynthesis. In some organisms, independent genes encode the pyrophosphohydrolase (HisE) and cyclohydrolase (HisI), while in eubacteria, these functions are fused into a single gene. Even more complex scenarios exist in certain eucaryotes such as yeast where the HisI−HisE functions are found on separate domains within a multifunctional enzyme containing the HisD domain (hisitdinol dehydrogenase) that catalyzes the final step in the histidine pathway (*6*).

† This work was supported by NIH Postdoctoral Fellowship F32GM18083 (R.L.D.) and NIH Grant RO1GM45756 (V.J.D.).

* To whom correspondence should be addressed. E-mail: vjd@pharmacy.purdue.edu.

‡ Current address: Department of Food Science, Cornell University, Stocking Hall, Ithaca, NY 14853-7201.

[1] Abbreviations: AAA, amino acid analysis; AAS, atomic absorption spectroscopy; Bis-Tris, bis(2-hydroxymethyl)iminotris(hydroxymethyl)-methane; Bis-Tris Propane, 1,3-bis[tris(hydroxymethyl)methylamino]-propane; CHES, 2-(*N*-cyclohexylamino)ethanesulfonic acid; ddH_2O, double-distilled deionized water; DEAE, diethylaminoethyl; DIPEAA, diisopropylethylamine acetate; DTT, dithiothreitol; EDTA, (ethylenedinitrilo)tetraacetic acid; HA, hydroxylapatite; ICP-ES, inductively coupled plasma emission spectroscopy; IPTG, isopropyl β-D-thiogalactopyranoside; HEPES, *N*-(2-hydroxyethyl)piperazine-*N*′-2-ethanesulfonic acid; HR-FABMS, high-resolution fast atom bombardment mass spectroscopy; MWCO, molecular weight cutoff; MALDI-MS, matrix-assisted laser desorption/ionization mass spectrometry; PCR, polymerase chain reaction; PR-AMP, N^1-(5′-phosphoribosyl)adenosine 5′-monophosphate; PRPP, 5-phosphoribosyl 1-pyrophosphate; 5′-Pro-FAR, N^1-[(5′-phosphoribulosyl)formimino]-5-aminocarboxamide ribonucleotide adenosine monophosphate; PVDF, polyvinylidene difluoride; SDS−PAGE, sodium dodecyl sulfate−polyacrylamide gel electrophoresis; SP-sepharose, sulfopropyl-sepharose; TAE, Tris-acetate EDTA; TBE, Tris-borate EDTA; TCEP, tris(2-carboxyethyl)phosphine; TFA, trifluoroacetic acid; Tris, tris(hydroxymethyl)aminomethane; TSP, 3-(trimethylsilyl)propionic-2,2,3,3-d_4 acid sodium salt; VB, Vogel Bonner.

10.1021/bi982475x CCC: $18.00
Published on Web 01/12/1999

Scheme 1: Conversion of PR-AMP to 5′-ProFAR by PR-AMP Cyclohydrolase

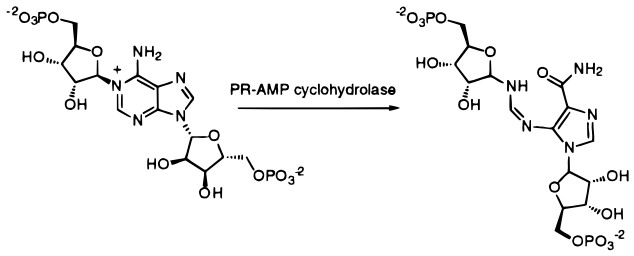

Incorporation of these enzymes into multifunctional systems has been associated with a regulatory function for gene expression especially in the case of yeast (*7*).

We have developed a recombinant form of N^1-(5′-phosphoribosyl)adenosine−5′-monophosphate cyclohydrolase from *Methanococcus vannielii* HisI for these studies because of its availability, high degree of homology with all known HisI enzymes, and its monofunctional character (*6*, *8*). This high-level production system has facilitated the first purification and characterization of any form of this unique enzyme. The synthesis of the substrate N^1-(5′-phosphoribosyl)adenosine 5′-monophosphate (PR-AMP) has been achieved by development of a second recombinant source of the functional enzymes, ATP phosphoribosyl transferase (HisG) and a N^1-(5′-phosphoribosyl)adenosine−5′-triphosphate phosphohydrolase (HisE) encoded by a single overproduction plasmid construct. A ready supply of substrate has facilitated the purification and direct UV−vis assay of the enzyme-catalyzed conversion of PR-AMP to 5′-ProFAR (*5*). PR-AMP cyclohydrolase appears to have a unique origin in histidine biosynthesis. The characterization of this enzyme is a first step in developing approaches toward potential inhibitors. The mechanism by which PR-AMP cyclohydrolase catalyzes this transformation is not known; however, the reaction is potentially related to those of other hydrolytic enzymes that use a Zn^{2+}-activated hydroxyl such as adenosine and cytidine deaminase (*9*, *10*).

MATERIALS AND METHODS

Materials. General biochemicals, buffers, and 1,10-phenanthroline were from Sigma/Aldrich. Inorganic pyrophosphatase was purchased from Boehringer Mannheim. Tris(2-carboxyethyl)phosphine (TCEP) was from Pierce. Zinc atomic absorption standard (1000 ppm) was from VWR. pET-28(b)+ and *Escherichia coli* BL21(DE3) cells were from Novagen. pBluescript II-SK(+)+ and *E. coli* XL-1 Blue were from Stratagene. Oligonucleotide primers were synthesized at the Purdue Center for Macromolecular Structure using an ABI automated synthesizer or purchased from Midland Certified Reagent Co. (Midland, TX). Qiagen DNA prep kits were purchased from Qiagen. Flexiprep DNA purification kits were purchased from Pharmacia. Restriction enzymes, T4 polymerase, and T4 ligase were from Promega, New England Biolabs, Stratagene, or U.S. Biochemical. Gene Clean II kits were from Bio101. Amplitaq was from Perkin-Elmer. Wizard PCR Preps and Taq DNA polymerase were from Promega. DEAE and SP-sepharose fast flow, Superose-12 HR 10/30, and Superdex-200 HR 16/60 gel filtration media were from Pharmacia. Hydroxylapatite was from Calbiochem. The Spectra/Por 4 12000−14000 MWCO membrane was from Spectrum, and 10000 MWCO Side-a-Lyzers were from Pierce. Chelex 100 (50−100 mesh), low-molecular weight range markers, and Bradford reagents were from Bio-Rad. Ultralow-molecular weight range SDS−PAGE markers were from Sigma. PVDF Immobilon-P transfer membranes, low-protein binding filters (0.22 and 0.45 μm), and Centricon and Centriprep concentrators were from Millipore.

General Methods. All procedures, restriction digests, transformation of *E. coli*, and general molecular biological manipulations were carried out using standard protocols (*11*, *12*). *E. coli* DH5α or XL-1 Blue (Stratagene) cells were used as host strains for propagation and isolation of plasmid DNA constructs. DNA sequence analysis of the *hisI* plasmids was performed at the Purdue DNA Sequencing Facility on a Pharmacia ALF Express Sequencer using fluorescent 5′Cy5 (Pharmacia) end-labeled primers (standard T7 or T3 primers) and cycle sequencing.

Protein sequence analysis was performed at the Purdue Center for Macromolecular Structure. Samples were separated by SDS−PAGE and transferred to PVDF membrane using a Bio-Rad Mini Trans-Blot apparatus before being subjected to Edman sequencing on an Applied Biosystems Procise 491 microsequencer.

Protein concentrations were determined with the method of Bradford (*13*) and corroborated by total amino acid analysis.

The SDS−PAGE was performed using Tris-Tricine gels (16.5% T and 3% C), without spacer gels, for visualization of lower-molecular weight proteins (*14*). Gels were fixed in a 5% glutaraldehyde solution to prevent diffusion of lower-molecular weight peptides before staining using the method described by Lloyd (*15*). Low-molecular weight range markers from Bio-Rad contained phosphorylase *b* (94 000 Da), bovine serum albumin (66 200 Da), ovalbumin (45 000 Da), carbonic anhydrase (31 000 Da), trypsin inhibitor (21 500 Da), and lysozyme (14 400 Da). Alternatively, ultralow-molecular weight range markers from Sigma contained triosephosphate isomerase (26 600 Da), myoglobin (17 000 Da), β-lactalbumin (14 200 Da), aprotinin (6500 Da), oxidized insulin chain B (3496 Da), and bradykinin (1060 Da). Densitometry analysis of gels was performed using a PDI Discovery Series Densitometer equipped with Quantity One Software.

Construction and Expression of phisGI(−)E-tac. Primer-adapted PCR was used to obtain the mutant *E. coli hisIE* gene from the genomic DNA of *E. coli* strain UTH903 [*hisI*(−)] (*15*). The primers were as follows: *hisIE* (sense), 5′-GAA TTC TGC AGG AGA TCA GGA TAT GTT AAC-3′; and *hisIE* (antisense), 5′-GGG AAG CTT ACT GAT GCC GTT TAC GCA GGT-3′. The sense primer contained the natural ribosome binding site AGGA (*16*), an *Eco*RI and *Pst*I site, and the antisense primer contained a *Hin*dIII site.

Each PCR mixture contained 1−100 ng of UTH903 genomic template DNA, 1.5 mM $MgCl_2$, 100−125 pmol of primers, 250 μM dNTPs, and 2.5 units of AmpliTaq polymerase in a 100 μL total volume and was overlaid with 100 μL of mineral oil. Thermal cycling conditions included 2.0 min at 94 °C, 1.0 min at 95 °C, 2.0 min at 42 °C, and 2.5 min at 72 °C; steps 2−4 were repeated for 35 cycles followed by a 5.0 min finishing step at 72 °C. The resultant PCR product was purified by phenol chloroform extraction, and analyzed by electrophoresis on a 1% agarose gel. The product was sequentially digested with *Pst*I and *Hin*dIII and

ligated into p*hisGIE-tac* (*16*) which had been digested with the same restriction enzymes and purified from an agarose gel using the Gene Clean kit (Bio101). Five clones which did not complement UTH903 [*hisI(−)*] were chosen for further analysis by overproduction of the HisG and HisI(−)E proteins. Transformation of *E. coli* FB1 cells with these five clones and subsequent SDS−PAGE analysis of soluble protein samples from induced cultures demonstrated overproduction of proteins with the expected molecular masses for HisG (33.2 kDa) and HisI(−)E (22.7 kDa).

Preparation of PR-AMP. Induced *E. coli* FB1 cells containing the p*hisGI(−)E-tac* plasmid described above were used to produce PR-AMP. Soluble protein extracts [HisGI(−)E] of these induced cells were prepared by ultrasonication followed by centrifugation to remove cellular debris and precipitation of ribonucleic acids with streptomycin sulfate (1.0%). In 30 mL of 230 mM Tris-HCl (pH 7.7), 1 mM EDTA, and 15 mM $MgCl_2$ were mixed PRPP (250 μmol), ATP (258 μmol), inorganic pyrophosphatase (∼0.4 unit/mL final concentration), and 3 mg of HisGI(−)E extract. The mixture was incubated at 30 °C for 3−4 h, and the reaction progress was monitored by the increase in absorbance at 290 nm for PR-AMP (ϵ_{290} = 2800 M^{-1} cm^{-1} at pH 7.5) (*5*) or by conversion of PR-AMP via HisI to 5′-ProFAR (ϵ_{300} = 6069 M^{-1} cm^{-1}) (*16*). The crude reaction mixture was diluted to 150 mL [with 10 mM imidazole hydrochloride (pH 6.5)], loaded onto a Q-Sepharose FF column (15.0 cm × 2.5 cm), and eluted using a linear gradient (5 mL/min) from 10 mM imidazole hydrochloride (pH 6.5) to 10 mM imidazole (pH 6.5) and 0.5 M LiCl over 900 mL. The PR-AMP (eluting at 285 mL into the gradient) was identified by UV−vis absorbance, and fractions with an A_{260}/A_{290} ratio of 6.5−8.0 [50 mM KH_2PO_4 (pH 7.5) and 1 mM EDTA] were pooled and dried by lyophilization. The white solid was triturated with 4 × 30 mL portions of ice-cold ethanol and dried by lyophilization again before storage at −20 °C. Typical yields for the process, as determined by absorbance of the pool at 290 nm, were 30−35%. PR-AMP concentrations for all samples were determined using the published extinction coefficient at 290 nm of 2800 M^{-1} cm^{-1} in 50 mM KH_2PO_4 (pH 7.5) and 1 mM EDTA (*5*). This extinction coefficient was verified by complete turnover of PR-AMP with HisI to 5′-ProFAR (ϵ_{300} = 6069 M^{-1} cm^{-1}) .

PR-AMP was analyzed by HPLC on a Hamilton PRP-1 column (250 mm × 4.1 mm) using isocratic elution at a rate of 1.0 mL/min with 25 mM diisopropylethylamine acetate (DIPEAA) (pH 7.0) and 2.5% CH_3CN. The retention times of PR-AMP, AMP, and ATP under these conditions were 6.9, 9.9, and 26.9 min, respectively: ^{1}H NMR of PR-AMP (500 MHz, D_2O; referenced to external TSP in D_2O) δ 8.63 (s, 1H), 8.44 (s, 1H), 6.27 (d, 1H, J = 3.2 Hz), 6.02 (d, 1H, J = 5.5 Hz), 4.69 (t, 1H, J = 5.4 Hz), 4.46 (m, 3H), 4.34 (bs, 2H), 4.13 (bm, 1H), 4.01 (m, 3H); ^{13}C NMR of PR-AMP (121 MHz, D_2O; referenced to external dioxane in D_2O) δ 150.3, 147.4, 145.2, 143.3, 119.6, 95.1, 88.3, 87.0, 84.9, 75.2, 72.9, 70.6 (2Cs), 64.0, 63.7; ^{31}P NMR of PR-AMP [300 MHz, 20% D_2O, 10 mM Bis-Tris Propane (pH 6.5), and 1 mM EDTA; referenced to external 10% H_3P0_4 in D_2O] δ 2.56 (s), 2.35 (s); HR-FABMS (−Ve glycerol) calcd 558.0639 $[M - H]^-$, observed 558.0663 $[M - H]^-$.

Determination of the pK_a of PR-AMP. The pK_a of the 6-amino group in PR-AMP was determined by analysis of the change in absorbance at 300 nm. Samples of PR-AMP (34 μM in 1 mL) were scanned at various pH values in the following buffers: 50 mM KH_2PO_4/NaOH (pH 11.3), 30 mM CHES/NaOH (pH 9.4 and 10.0), 30 mM Bis-Tris Propane-HCl (pH 9.0, 8.6, 8.0, 7.5, 7.1, and 6.5), and 30 mM Bis-Tris-HCl (pH 6.0). The data for the PR-AMP pK_a were fitted using eq 1 for a single pK_a:

$$Y = \frac{L_1 + L_2[10^{(\mathrm{pH}-\mathrm{p}K_a)}]}{[10^{(\mathrm{pH}-\mathrm{p}K_a)} + 1]} \quad (1)$$

where Y is equal to the change in absorbance at 300 nm and L_1 and L_2 represent the lower and upper limits of the function, respectively.

Construction of phisI-T7-ΔTag. Primer-adapted PCR was used to obtain the *M. vannielii hisI* gene from the pET-921 plasmid (*6*). The primers, with restriction sites in noncoding regions, were as follows: *M. vannielii hisI* (sense), 5′-GCA TGA ATT CAT ATG GGC ATT AAA GAC ATT-3′; and *hisI* (antisense), 5′-GGG CAA GCT TCA TTA ATC TAG TTT ATC TCC-3′. These primers were designed with *Eco*RI and *Nde*I sites and a start codon in the sense primer and a *Hin*dIII site and stop codon in the antisense primer.

The PCR mixtures contained 0.1−10 ng of template DNA, 1.5−3.0 mM $MgCl_2$, 150−200 pmol of primers, 200−250 μM dNTPs, and 2.5 units of AmpliTaq polymerase (using Perkin-Elmer-supplied buffer) or 2.5 units of Promega Taq polymerase, in a 100 μL total volume overlaid with 75 μL of mineral oil. All thermal cycling was performed using a PC-100 thermal cycler (MJ research). Thermal cycling steps included 30 s at 94 °C, 2.0 min at 55 °C, and 2.5 min at 72 °C for 30 cycles, followed by a 10 min extension step at 72 °C. PCR products were analyzed by 1.5% agarose gel in TAE buffer and purified by Wizard PCR Preps. The resulting products were digested with *Eco*RI and *Hin*dIII and cloned into pBluescript II-SK(+). Plasmids containing *M. vannielii hisI* were functionally verified by their ability to confer growth to *E. coli* UTH903 [*hisI(−)*] on VB minimal media. DNA sequence analysis confirmed the desired *hisI* coding sequence for the plasmid, p*hisI*-SK. The *Nde*I−*Hin*dIII restriction fragment from p*hisI*-SK was separated on a 1.5% TAE agarose gel, excised, and purified using the Gene Clean Bio101 kit. Ligation of this fragment into the *Nde*I and *Hin*dIII sites of pET-28(b)+ created an N-terminal His tag fusion with HisI. The recombinants were screened for the insert DNA using the same restriction enzymes to identify an appropriate clone named p*hisI-T7*-tag.

The His tag leader sequence from p*hisI-T7*-tag was deleted by digestion with *Nco*I and *Nde*I and extension with T4 DNA polymerase, followed by blunt end ligation with T4 DNA ligase. The desired clone p*hisI-T7*-Δtag (His tag eliminated) was initially identified by *Xba*I−*Hin*dIII restriction analysis on analytical agarose gels. The clone was subsequently analyzed with DNA sequencing to confirm the integrity of the *hisI* gene.

Overproduction of PR-AMP Cyclohydrolase. E. coli BL21-(DE3) cells were freshly transformed with p*hisI*-T7-Δtag (*12*) by selection on LB/kanamycin (30 μg/mL) plates at 37 °C for 12 h. Single colonies were used to inoculate 3 mL cultures and allowed to grow for 8−12 h before inoculating 25 mL of fresh LB/kanamycin with the entire 3 mL culture and growth for another 12−16 h. The culture was then transferred

to 1 L of LB/kanamycin and grown to OD_{550nm} of 0.9 before induction by addition of 1 mM IPTG. Cells were grown for 4−5 h beyond induction to the stationary phase (OD_{550nm} = 3.5), harvested by centrifugation, and stored at −80 °C.

Purification of PR-AMP Cyclohydrolase. Purification was carried out at 4 °C unless otherwise noted, and buffers were prepared at room temperature. Induced *E. coli* BL21(DE3) cells (1 L) containing *phisI*-T7-Δtag were allowed to thaw on ice in 10 mL of 50 mM Tris-HCl (pH 7.5) and 250 mM NaCl with 5 mM $ZnCl_2$ and lysed by ultrasonication using a Branson model 250 sonifier. This sample was diluted to 20 mL with 50 mM Tris-HCl (pH 7.5) and centrifuged at 11000*g* for 15 min. The supernatant was made 1.2% in streptomycin sulfate, incubated for 15 min on ice, and centrifuged at 11000*g* for 15 min. The resulting supernatant was diluted to 45 mL with 50 mM Tris-HCl (pH 7.5) and loaded directly onto DEAE Sepharose FF (5 cm × 5 cm) and SP Sepharose FF (15 cm × 2.5 cm) columns linked in series at a flow rate of 5.0 mL/min. PR-AMP cyclohydrolase was collected in the flow through (100 mL) before loading directly onto an hydroxylapatite (HA) column (4.0 cm × 2.5 cm). The column was washed with 4 volumes of 10 mM KH_2PO_4 (pH 7.5), and the protein was eluted with a linear gradient in phosphate made with 200 mL of 10 mM KH_2PO_4 (pH 7.5) and 200 mL of 400 mM KH_2PO_4 (pH 7.5). HisI eluted from 100 to 120 mL into the gradient, and fractions with a specific activity of ≥16.0 units/mg were pooled, filtered through a 0.22 μm low-protein binding filter into a sterile vial, and stored at 4 °C. Enzyme activity was stable at this point for 1 month. Longer-term storage of PR-AMP cyclohydrolase was achieved by concentrating to 1−2 mg/mL using a Centriprep 10, precipitating by adding polyethylene glycol (PEG) 3350 (31% final concentration), followed by $MgCl_2$ (10 mM final concentration), and centrifuging at 12000*g*. The resultant pellet was stored at −20 °C until it was used.

Protein Analysis. A total protein analysis was carried out on multiple samples of purified HisI. The observed difference between the Bradford analysis and total protein amino acid analysis (AAA) was +9.5%, with AAA giving the higher value. Protein concentrations reported here are based on the Bradford analysis.

PR-AMP Cyclohydrolase Assay and Kinetic Constants. The cyclohydrolase assay was based upon the $\Delta\epsilon_{300nm}$ of 6700 M^{-1} cm^{-1} at pH 7.5 (or a $\Delta\epsilon_{260nm}$ of 8020 M^{-1} cm^{-1} at pH 7.5) for the conversion of PR-AMP to 5′-ProFAR (see Figure 1). These extinction coefficients were determined by subtraction of the starting absorbance value at 300 or 260 nm from the final absorbance value after complete turnover of known concentrations of PR-AMP (23.5, 50.7, and 61 μM) by PR-AMP cyclohydrolase. Routine assays were conducted at 30 °C in a Varian CARY 3 UV−vis spectrophotometer in a total volume of 1 mL with either 30 mM HEPES (Chelex-treated) (pH 7.5) or 50 mM Tris-HCl (pH 7.5) and 1 mM EDTA with 5 mM $MgCl_2$ and 50 μM PR-AMP. Reactions were initiated by adding 0.1−0.2 μg of PR-AMP cyclohydrolase.

The determination of steady state kinetic constants was performed in Chelex-treated 30 mM HEPES (pH 7.5) and 1.0 mM $MgCl_2$ at 30 °C with PR-AMP concentrations being varied from 0.96 to 48 μM. All determinations were performed in triplicate on a Varian CARY 4 UV−vis spectrophotometer, and the initial rates were estimated over the first 1.0−2.0 min. Determination of the k_{cat}/K_m pH profile was carried out in 30 mM Bis-Tris Propane-HCl (pH 9.0, 8.6, 8.0, 7.5, 7.1, and 6.5) and 30 mM Bis-Tris-HCl (pH 6.0). Substrate saturation curves at each pH value were defined by a minimum of eight substrate concentrations over the range of 0.5−48 μM PR-AMP with observation at 260 nm ($\Delta\epsilon_{260nm}$ = 8020 M^{-1} cm^{-1}) and 5.0 mM $MgCl_2$. Values for the steady state kinetic parameters were calculated, with no weighting applied, using the Michaelis−Menten hyperbolic model, and the k_{cat}/K_m data were fit as a function of pH (Origin 5.0, Microcal Software, Inc.) using the model described above (eq 1).

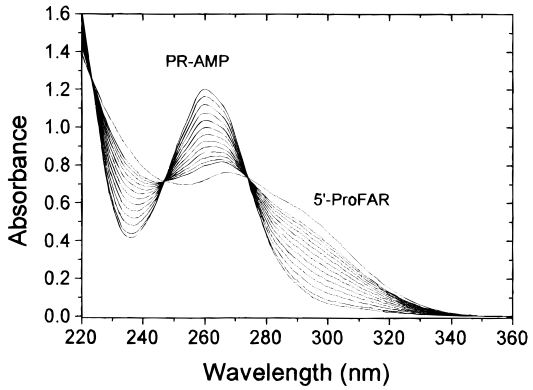

FIGURE 1: Conversion of PR-AMP to 4′-ProFAR. Full spectrum of the conversion of PR-AMP to 5′-ProFAR at 30 °C in 50 mM Tris-HCl, 10 mM $MgCl_2$ (pH 7.5), 0.8 mg of PR-AMP cyclohydrolase, and 61 mM PR-AMP. Spectra were acquired every 2.0 min after addition of enzyme, and the final spectrum was obtained at 24 min. Isosbestic points are observed at 223, 247, and 274 nm.

Effect of Free Magnesium and Zinc on Activity. All experiments were performed in Chelex 100-treated 30 mM HEPES (pH 7.5) at 30 °C, and duplicate initial rate measurements were conducted. All PR-AMP cyclohydrolase solutions were dialyzed versus the same buffer with Chelex 100 (4 g/L) for 24 h. All PR-AMP samples were titrated to pH 4.5 with dilute HCl and passed through a column (10 mm × 30 mm) of Chelex 100 to remove adventitious metals. The apparent steady state K_s for Mg^{2+} was determined in experiments where a constant amount of enzyme (0.22 μg) was used to initiate the reactions in which PR-AMP (51 μM) and Mg^{2+} (1−200 μM) were preincubated in 1 mL. The background rate for these experiments in the absence of Mg^{2+} was less than 5% specific activity.

EDTA was used as an inhibitor of PR-AMP cyclohydrolase to demonstrate the requirement for free Mg^{2+}. PR-AMP cyclohydrolase (1.0 μg) was added to assay preincubation mixtures containing Mg^{2+} (150, 250, or 350 μM), PR-AMP (72 μM), and varying amounts of EDTA (0−550 μM). Initial rate measurements were assessed in the first 30−40 s after mixing, and the fractional activity was plotted as a function of EDTA concentration. The IC_{50} of Zn^{2+} for PR-AMP cyclohydrolase was determined by varying free Zn^{2+} concentrations (0−40 μM) under conditions of constant PR-AMP (72 μM) and Mg^{2+} (1.0 or 10 mM). The fractional activity was plotted as a function of Zn^{2+} concentration.

Gel Filtration. Gel filtration chromatography (at room temperature) on a Superdex 200 HR 16/60 column was

performed in 50 mM Tris-HCl (pH 7.5), 1 mM EDTA, and 500 mM NaCl at a flow rate of 0.75 mL/min. The void volume of the column was determined to be 36 mL with a total bed volume of 122 mL. Catalase (232 000 Da, elution volume of 66.1 mL), aldolase (158 000 Da, 68.3 mL), bovine serum albumin (67 000 Da, 77.4 mL), and chymotrypsinogen A (25 000 Da, 93.9 mL) were used as molecular mass standards under the same conditions (*17*).

Analytical Ultracentrifugation. Sedimentation equilibrium analysis of purified PR-AMP cyclohydrolase was performed on a Beckman XL-A analytical ultracentrifuge. Three samples of HisI (0.2, 0.6, and 0.6 mg/mL with 0.5 mM EDTA) were analyzed (275 nm) by sedimentation equilibrium in 50 mM Tris-HCl (pH 7.5) and 500 mM NaCl at 20 000 rpm for 16−20 h at 20 °C. The liquid column size was 3 mm, and the partial specific volume of solute (vbar = 0.743 mL/g), based on the monomeric HisI amino acid sequence, was calculated using Sednterp (*18*). The density (ρ = 1.02 g/mL) of the solution was calculated using the same program with the buffer conditions, ionic strength, and temperature as described above. These values were used for data analysis and fitting with Sedeq1b (*19*) to a nonequilibrium model for two species (initial estimates of 25 and 64 kDa) that were allowed to float during fitting iterations.

Metal Ion Analysis. Samples of PR-AMP cyclohydrolase for metal ion analyses via inductively coupled plasma emission spectroscopy (ICP-ES) (20 metals, Al, B, Ba, Ca, Cd, Co, Cr, Cu, Fe, K, Mg, Mn, Mo, Na, Ni, P, Pb, Si, Sr, and Zn) and atomic absorption spectroscopy (AAS) for Zn were prepared by extensive dialysis at 4 °C for 2−3 days. Up to 10 mg of protein at 1.0 mg/mL was dialyzed against 400 mL of 30 mM HEPES (pH 7.5) containing 4 g/L Chelex 100 (50−100 mesh) resin for 6−8 h, with changes after 12−16 h (2 L) and 30−34 h (2 L). The Spectra/Por 4 12000−14000 MWCO dialysis membrane was prepared according to standard procedures (*20*) and rinsed with HEPES buffer prepared by stirring with 4 g/L Chelex 100 for 24 h before use. All HEPES solutions were made from the sodium salt and titrated with NaOH to pH 7.5, and the Chelex 100 used in these preparations was regenerated to the sodium form. All containers (plastic and glassware) were triple rinsed or soaked in HEPES containing Chelex 100 (4 g/L), and plastic materials were used whenever possible. As a control to correct for any matrix effects, a standard curve was constructed with known quantities of Zn^{2+} from a reference solution of zinc nitrate. ICP-ES samples (1.5−2.0 mL, 0.5−1.0 mg/mL) were analyzed at the Chemical Analysis Laboratory (University of Georgia, Athens, GA), and AAS samples (7 mL, 0.25−0.65 mg/mL) were analyzed at the Indiana State Chemist's Laboratory (Purdue University).

1,10-Phenanthroline Dialysis. Preparation of apo-PR-AMP cyclohydrolase (500 μL at 1.1 mg/mL) was conducted in 10000 MWCO Side-a-Lyzers (Pierce) by dialysis against 1 L of 30 mM HEPES (pH 7.5) and 5 mM 1,10-phenanthroline, in the presence of 3 g/L Chelex 100 (50−100 mesh) (*21*). The PR-AMP cyclohydrolase activity was sampled over 24 h until the residual specific activity remained constant at 3%. These samples were further dialyzed against Chelex 100-treated HEPES prepared as described above, to remove 1,10-phenanthroline before submission of triplicate samples for ICP-ES analysis. Control dialyses were performed in the absence of 1,10-phenanthroline.

Table 1: Purification of *M. vannielii* PR-AMP Cyclohydrolase

purification step	volume (mL)	protein (mg)	activity (units/mg)	units	% yield
crude extract	23	253	6.8	1720	100
streptomycin (1.2%)	43	232	7.2	1670	97
DEAE-SP-sepharose	110	98	11.3	1107	64
hydroxylapatite	40	43	17.6	756	44

RESULTS

Preliminary HisI Studies. Our preliminary studies with the bifunctional *E. coli* HisIE protein and the mutant strain UTH903 [*hisI(−)*] were directed at the production of PR-AMP. Protein extracts from induced *E. coli* FB1 cells containing the *phisGI(−)E-tac* plasmid provided an efficient source of PR-AMP starting with PRPP and ATP. No evidence was observed for additional nucleotide intermediates in these substrate preparations. These initial investigations highlighted the potential intricacy of the bifunctional protein activities. Furthermore, truncation mutants of the HisE functional domain at D129 (based on alignment data that suggested separation of active site domains) provided a functional HisI protein that was overproduced and purified (data not shown). Complementation experiments have demonstrated that this construct contained a functional HisI protein, and the overproduced purified protein displayed catalytic activity. However, the circumspect stability of this mutant as the His tag affinity-purified protein, and the discovery of additional metal cofactor requirements, highlighted the complexity of the multifunctional *E. coli* HisIE enzyme. These observations motivated a more focused effort on the native monofunctional HisI from *M. vannielii* (*6*).

Overproduction and Purification. The *M. vannielii hisI* gene was originally subcloned from the pET-921 plasmid (*6*) into pET-28(b)+ to take advantage of the His tag leader sequence for Ni^{2+} affinity purification and hasten the examination of the purified enzyme. The subsequent difficulty in the removal of the His tag leader sequence in the fusion protein, the discovery of metal cofactors, and the sensitivity to thiol reagents led to the removal of the His tag coding DNA to produce native HisI in the same vector. Expression of the *hisI* gene in this plasmid construct harbored in *E. coli* BL21(DE3) cells provided an efficient source of PR-AMP cyclohydrolase. Protein purification was optimized by the addition of $ZnCl_2$ to the lysis buffer and the use of two negative chromatographies (DEAE and SP Sepahrose) followed by elution from hydroxylapatite (HA) as summarized in Table 1. The protein in the final preparation showed two minor and one major species that together constitute >95% of the isolated protein as determined by scanning densitometry analysis of the Coomassie blue-stained SDS−PAGE gel (Figure 2). All of these bands were determined to have the same N-terminal sequence as *M. vannielii* HisI. The purified enzyme was analyzed by N-terminal sequencing and lacked an N-terminal methionine, while the next 25 amino acids were an exact match for the known primary sequence of the *M. vannielii* HisI protein.

The molecular mass of the isolated (major band) protein was estimated to be 15 200 Da by SDS−PAGE, and three major molecular ions were observed in the MALDI-MS (*22*) spectrum of HisI: 15 486, 10 698, and 4818, respectively. The largest molecular weight observed was consistent with the calculated value of 15 490.1 for the protein lacking an

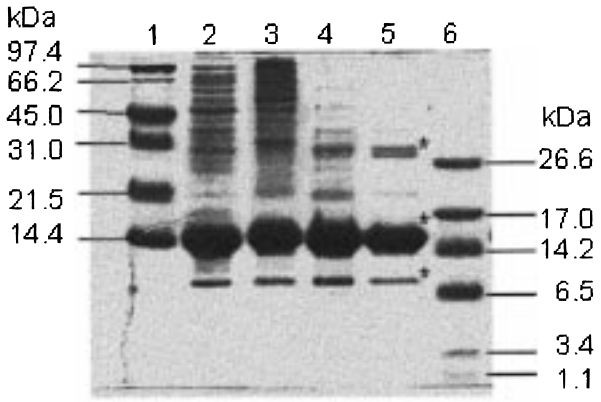

FIGURE 2: Purification of PR-AMP cyclohydrolase via Tris-Tricine SDS−PAGE analysis: lane 1, molecular weight markers from Bio-Rad; lane 2, crude extract; lane 3, streptomycin cut; lane 4, DEAE-SP-sepharose; lane 5, HA fraction; and lane 6, molecular weight markers from Sigma. In the crude extract (lane 2), the dominant band is 40% of the total protein, and in lane 5, this band is 86% of the total protein in that lane as calculated by densitometry analysis. Bands marked with an asterisk (*) in lane 5 have the same N-terminal sequence.

N-terminal methionine. Also observed was a variable amount of lower-molecular weight species (5−15% of the total purified protein) that also had the same N-terminal sequence as *M. vannielii* HisI and had a molecular weight of 10 698 as determined by MALDI-MS analysis. This fragment corresponded to residues 2−92 (calculated weight of 10 690.7) of HisI. The smaller fragment corresponded to residues 93−136 (calculated weight of 4819.0). The sum of the experimental results for these fragments was 15 516, which is consistent with the subunit mass of HisI. Finally, a dimeric (36.9 kDa) species was detected on the SDS−PAGE gels in ca. 8−16% of the purified total protein based on scanning densitometry. N-Terminal sequencing of the dimeric species indicated that it had an N-terminal sequence identical to that of *M. vannielii* HisI. This species was not observed with MALDI-MS.

Native Molecular Weight. PR-AMP cyclohydrolase was analyzed by gel filtration chromatography on a Superdex 200 HR 16/60 column. The major peak eluted at a volume (88.5 mL) that was consistent with a dimer (34 kDa) and exhibited PR-AMP cyclohydrolase activity. This result was consistent with the observation of a dimeric species on SDS−PAGE. Also present in the gel filtration experiments was a smaller amount (12%) of oligomeric material eluting at 77.8 mL that represented a pentamer (79 kDa). This form of HisI showed 50% of the specific activity of the dimeric species. The elution volumes of the protein standards and PR-AMP cyclohydrolase were the same whether EDTA was included in the buffer.

Analytical ultracentrifugation was also employed to determine the molecular weight of PR-AMP cyclohydrolase. The data from three independent sedimentation equilibrium runs were fitted to a nonequilibrium model that converged on average molecular weights for two species of 31 200 (86%) and 75 800 (14%). These values were consistent with those obtained by gel filtration as described above, and confirmed that the major form of the enzyme under these conditions is a dimer with an observed molecular weight of 31 200 (calculated molecular weight of 30 980).

Metal Ion Analysis. PR-AMP cyclohydrolase samples were analyzed for metal content by both ICP-ES and AAS. The

Table 2: Summary of Zinc Data[a]

enzyme	Zn^{2+} (mol/subunit)	protein (μM)	method
PR-AMP cyclohydrolase	1.1 (0.88, 1.07)	66 (27, 20)	ICP-ES (AAS)

[a] Average for all samples = 1.02 ± 0.12.

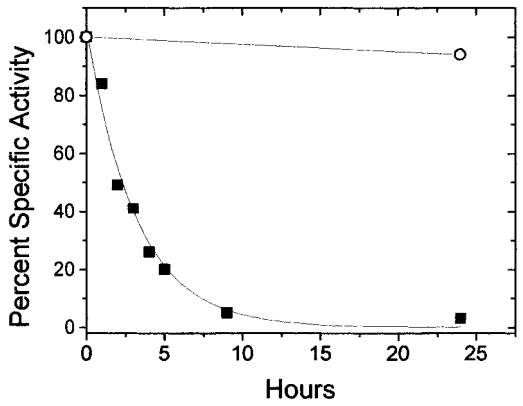

FIGURE 3: Inhibition of PR-AMP cyclohydrolase by zinc: (■) 1.0 mM Mg^{2+} and (○) 10 mM Mg^{2+}. The apparent IC_{50} values for zinc are 3.4 (1.0 mM Mg^{2+}) and 5.6 μM (10 mM Mg^{2+}).

molar ratio of Zn^{2+} to enzyme was consistent with the presence of a single tightly bound Zn^{2+} per subunit in the active enzyme preparations (Table 2). All other metals (excluding sodium), including Mg^{2+}, were either absent or present in quantities of <10% (total) stoichiometry. Purification in the presence of EDTA (1 mM) did not remove the Zn^{2+} from the enzyme, and neither did extensive dialysis against Chelex 100. However, dialysis of PR-AMP cyclohydrolase against 1,10-phenanthroline (Zn^{2+} specific chelator) inactivated the enzyme (see Figure 3). The enzyme samples treated in this fashion were found to contain negligible Zn^{2+} (<0.07 equiv). Enzyme which had been inactivated by dialysis against 1,10-phenanthroline resisted reactivation beyond about 50% of the original specific activity by reduction with TCEP (*23*) and addition of Zn^{2+}.

PR-AMP Cyclohydrolase Assay and Kinetic Constants. A procedure for the synthesis and purification of the substrate, PR-AMP, was developed on the basis of a strategy previously implemented to produce other histidine biosynthetic intermediates (*16*). This method offered a reliable, one-step preparation of substrate from PRPP and ATP and enabled the development of a UV−vis assay for PR-AMP cyclohydrolase activity. Figure 1 shows a full spectrum time course for the conversion of PR-AMP to 5′-ProFAR. An absolute requirement for exogenous Mg^{2+} in this reaction was observed. Other metals tested (Mn^{2+}, Ca^{2+}, and Zn^{2+}) would not support the catalytic activity under the same assay conditions. PR-AMP cyclohydrolase activity was found to be equivalent in several buffers, containing 1.0−10 mM $MgCl_2$, including 50 mM Tris-HCl (pH 7.5), 1 mM EDTA, 30 mM HEPES (Chelex-treated) (pH 7.5), and 50 mM KH_2PO_4 (pH 7.5) and 1 mM EDTA.

The Mg^{2+} requirement of PR-AMP cyclohydrolase is demonstrated in Figure 4. Panel A shows the inhibitory effect of increasing EDTA concentrations on the catalytic activity. The IC_{50} for EDTA (ranging from 188 to 389 μM) increased as a function of Mg^{2+} concentration. Panel B shows the fractional PR-AMP cyclohydrolase activity as a function of the EDTA:Mg^{2+} ratio present in the assay. At ca. 1.2 equiv

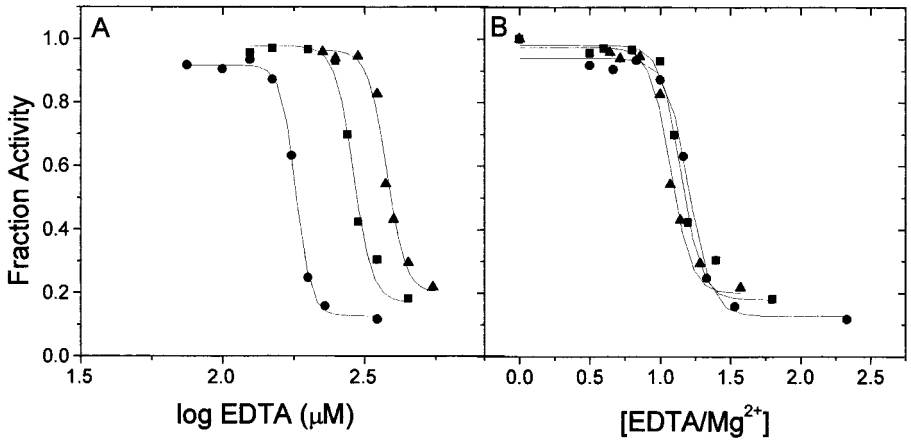

FIGURE 4: Demonstration of the Mg^{2+} requirement of PR-AMP cyclohydrolase. (A) Data plotted as the log of the EDTA concentration demonstrating that the amount of EDTA added must be increased as a function of Mg^{2+} concentration to obtain inhibition. $IC_{50} = 181$ (150 μM Mg^{2+}), 289 (250 μM Mg^{2+}), and 380 μM (350 μM Mg^{2+}). (B) Inhibition of activity with respect to the ratio of EDTA to Mg^{2+} present in the assay. At 1.2 equiv of EDTA to Mg^{2+}, there is a 50% loss of activity. The PR-AMP concentration was constant for all reactions (72 μM): (●) 150 μM Mg^{2+}, (■) 250 μM Mg^{2+}, and (▲) 350 μM Mg^{2+}.

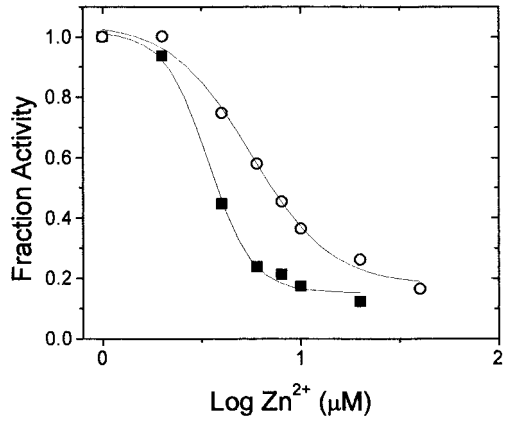

FIGURE 5: Dialysis of PR-AMP cyclohydrolase against 1,10-phenanthroline. Data were fit to a single-exponential decay, and the estimated rate constant was 9×10^{-5} s^{-1}. The line (○) represents data from a control dialysis in the absence of 1,10-phenanthroline.

of EDTA to Mg^{2+}, there is a 50% loss of activity at all concentrations of Mg^{2+}. The average free concentration of Mg^{2+} at this point was calculated to be 3.1 μM (*24*), a value consistent with one estimated from the dissociation constant ($K_s = 4.9 \pm 0.7$ μM) for Mg^{2+}. Inhibition was reversible as full activity was regained by the addition of excess Mg^{2+}. These data indicate that free Mg^{2+} is required for activity of PR-AMP cyclohydrolase. Interestingly, inclusion of Zn^{2+} in assays with Mg^{2+} did not activate the enzyme; moreover, small amounts (3−5 μM) of free Zn^{2+} strongly inhibited the enzyme as shown in Figure 5. This inhibition was also reversed by the addition of an equivalent amount of EDTA and excess Mg^{2+} and distinguishing this metal binding site from the high-affinity Zn^{2+} site.

Kinetic Constants and pH Profile. The steady state kinetic constants were determined for purified PR-AMP cyclohydrolase as follows: $K_m = 9.9 \pm 1.7$ μM and $k_{cat} = 4.1 \pm 0.3$ s^{-1} ($k_{cat}/K_m = 4.1 \times 10^5$ M^{-1} s^{-1}) at pH 7.5 and 30 °C. In Figure 6A, the absorbance of PR-AMP at 300 nm is plotted with respect to pH. This change in absorbance reflects the deprotonation of the 6-amino group of PR-AMP as shown in Scheme 2. The data were fitted to eq 1 to estimate a pK_a of 8.8 ± 0.1. This value is in good agreement with that reported (ca. 8.5) by Smith and Ames (*5*). The maximum turnover for PR-AMP cyclohydrolase occurs at pH 7.5 (Figure 6B), and the k_{cat}/K_m profile[2] (Figure 6D) showed a single pK_a of 7.3 ± 0.1. This value is 1.5 pK_a units from that determined for the substrate PR-AMP, indicating that the substrate protonation state is not complicating the interpretation of the pH−rate profile.

DISCUSSION

PR-AMP cyclohydrolase represents a link between a catabolic and metabolic process by catalyzing a step that initiates redistribution of carbon and nitrogen from ATP into the amino acid histidine. The global primary amino acid sequence comparisons (*6*, *8*) of HisI indicate a unique origin for this protein in histidine biosynthesis. There are several highly conserved regions in all forms of the protein, and functional analysis of the archael enzyme serves as a basis for understanding their roles. The focus of this work was to analyze the basic catalytic properties, cofactor requirements, and physical parameters of the *M. vannielii* enzyme.

PR-AMP cyclohydrolase binds a single Zn^{2+} per subunit (1:1 molar ratio), and these studies have established that this protein is a metalloenzyme. ICP-MS multiple-metal analysis demonstrated that only Zn^{2+} was bound in stoichiometric quantities to the PR-AMP cyclohydrolase preparations. During initial purifications of PR-AMP cyclohydrolase, it was discovered that addition of Zn^{2+} to the lysis buffer enhanced the specific activity and stability of the protein. However, different preparations of PR-AMP cyclohydrolase for ICP-ES and AAS studies indicated that the specific activity of the enzyme was not directly related to the zinc content, since preparations ranging from 9.0 to 18 units/mg contained the same amount of zinc bound per subunit. Apparently, a second process other than loss of zinc was responsible for inactivation and, hence, the lower specific activity of these preparations. The Zn^{2+} is tightly bound with an estimated K_d of $\leq 5 \times 10^{-9}$ based on the 1,10-phenanthroline dialysis experiments. It is probable that this metal plays at least a cocatalytic role in this enzyme (see below). However, additional roles for the Zn^{2+} include a structural one since there are conserved cysteine residues implicated by the primary sequence data for HisI. The region including

[2] Conditions for determination of K_m and k_{cat} described in the text were different from those described in the k_{cat}/K_m profile in Figure 6.

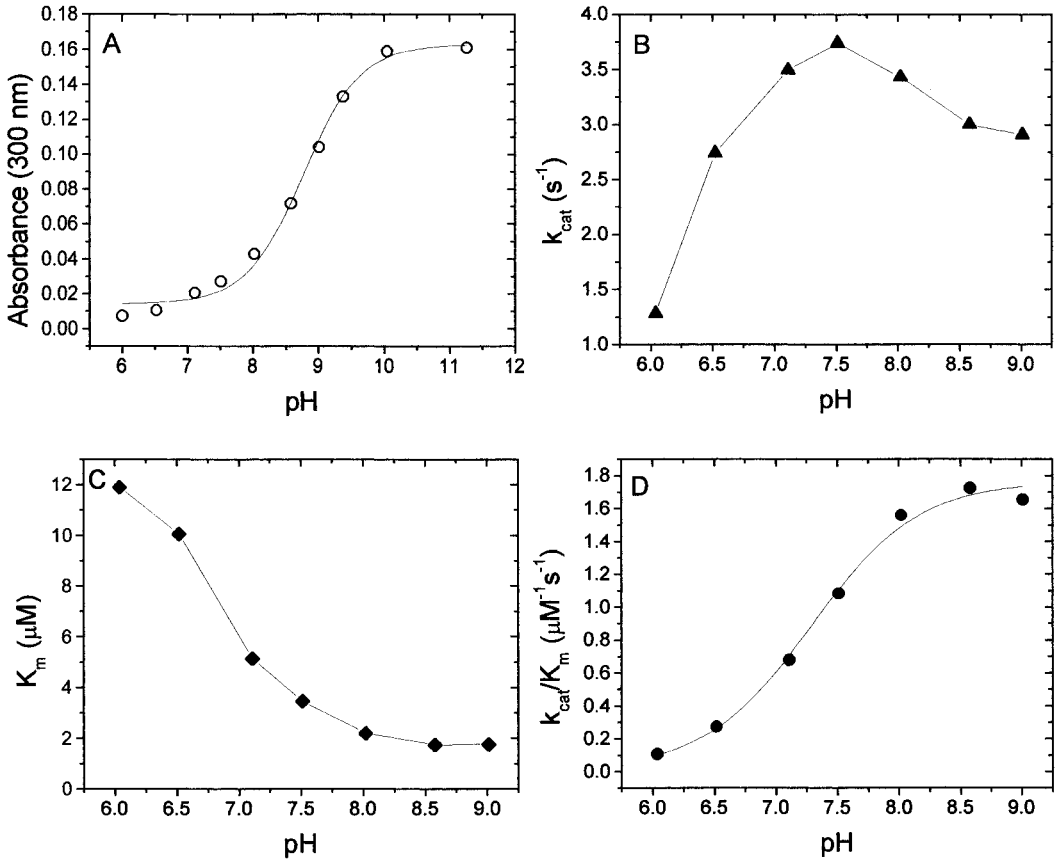

FIGURE 6: Dependence of PR-AMP absorbance (300 nm) on pH (A) and the pH−rate profile for PR-AMP cyclohydrolase activity (B−D).

Scheme 2: pK_a of the 6-Amino Group of PR-AMP

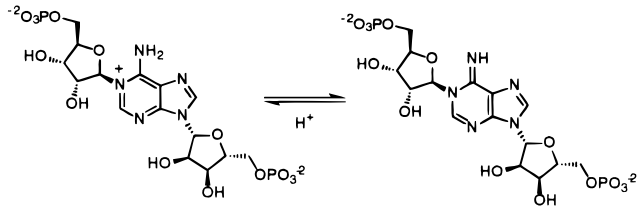

$C^{93}(X)_{15}C^{109}H^{110}(X)_5C^{116}$ suggests a unique motif that shows a high probability for a Zn^{2+} binding domain. When compared to known structural Zn^{2+} sites in proteins, cysteine−sulfur ligands prevail as a common paradigm (*25*−*27*).

A property related to the metal binding appears to be an intrinsic instability of the protein. The major bands that appear on SDS−PAGE (Figure 2) for the protein purified from *E. coli* show materials at masses of 31, 15, and 10 kDa that have been identified by N-terminal sequencing and MALDI-MS analysis to be derived from the *M. vannielii* PR-AMP cyclohydrolase. One possible explanation for these results is that the fragments are a result of "self-catalyzed" degradation and dimer formation. MALDI-MS data indicated that the position of the major cleavage occurs adjacent to the highly conserved C^{93} to produce a fragment with a MW of 10 697. The sequence context is VEKD/CDGDAL; there are no known protease sites in *E. coli* for this position (*28*). The fragmentation may have resulted from an oxidative (hydroxyl radical-mediated) cleavage event, and we have observed an increase in the accumulation of this cleaved protein in the presence of Fe^{2+} (unpublished results). This type of cleavage has precedent (*29*, *30*) and implicates the conserved amino acids at D92 and/or C93 as potential metal binding residues. Although less likely, an alternative cleavage at this position may represent the hydrolysis of a thioester formed by rearrangement of the amide backbone (*31*, *32*).

A second, lower-affinity metal binding site for Mg^{2+} must exist in the presence of the substrate PR-AMP. ICP-ES analyses demonstrated that Mg^{2+} was not observed in these preparations in amounts greater than 10% of the protein stoichiometry. In the early stages of this study, a requirement for Mg^{2+} in our assay mixture for PR-AMP cyclohydrolase was observed. A related observation was made with the enzyme activities for the bifunctional HisIE enzyme of *Salmonella typhimurium*, but was attributed to only the HisE or phosphohydrolase function (*5*, *33*).

The experimental results and amino acid sequence alignments are consistent with a model for cobinding of the substrate and metal cofactor (Mg^{2+}) to cyclohydrolase. The steady state kinetic analysis indicated that PR-AMP cyclohydrolase has a significant Mg^{2+} affinity (K_s = 4.9 μM) which is comparable to the K_m for substrate PR-AMP. However, this binding model would exclude the preassociation of Mg^{2+} and PR-AMP. All of the data related to metal binding indicate that free Mg^{2+} is required for full activity. Competition for the protein-bound Zn^{2+} by EDTA was ruled out since samples of PR-AMP cyclohydrolase incubated in the presence of 1 mM EDTA were "reactivated" by the addition of excess Mg^{2+} without addition of Zn^{2+}. Finally, Mg^{2+} is not expected to show significant affinity for free PR-AMP since the relative association constants for association with related adenosine nucleotides AMP, ADP, and ATP (*34*) are distinct ($>10^2$) from the range of K_s values observed.

The substrate specificity and cofactor requirements for PR-AMP cyclohydrolase are supported by the amino acid sequence analysis. There are two related motifs with functional relationships to enzyme substrate binding for hexoses or pentoses and nucleotide phosphoesters that all involve Mg^{2+} (*35*, *36*). A similar motif is evident for all PR-AMP cyclohydrolases based on sequence alignments. The consensus sequences for these motifs vary in length and are generally rich in glycine, lysine, and serine (threonine) (*36*, *37*). In PR-AMP cyclohyrolases, the region defined by S^{67}R-[ST]RXX[LI]WXKG[EA]TSG^{81} (using *M. vannielii* numbers) represents a consensus sequence that would constitute a "P-loop type" region associated with Mg^{2+}−phosphate binding.

Another distinctive feature of the PR-AMP cyclohydrolase is related to the active site functional group. The pH−rate analysis presented in this paper covers the region of pH 6.0−9.0 and defines a single protein-associated pK_a of 7.3. PR-AMP has a pK_a of 8.8 that is distinct from that defined by the enzyme pH−rate profile by 1.5 pK_a units. Others have speculated that the species are conserved residues His (110) and Cys (93, 109, or 116) or a Zn^{2+}-bound H_2O (*38*, *39*). Other possible mechanistic paths for the cyclohydrolase would be related to those found in metalloproteaeses (*40*), given the invariant histidine and the highly conserved aspartate residues at positions 92, 94, and 96. The catalytic reaction and the specific roles for these conserved amino acids will be the subject of continued study.

Therefore, PR-AMP cyclohydrolase utilizes both Zn^{2+} and Mg^{2+} in the hydrolysis of PR-AMP between N1 and C6, a reaction unique to histidine biosynthesis. From a mechanistic perspective, the reaction catalyzed by PR-AMP cyclohydrolase is analogous to those catalyzed by adenosine deaminase (*10*), AMP deaminase (*41*), and cytidine deaminase (*9*). These enzymes catalyze deamination by direct attack of a metal (Zn^{2+})-activated water molecule through an addition−elimination mechanism. However, there are clear distinctions in the activation barriers for selective hydrolysis of the N1−C6 bond in PR-AMP since this reaction pathway has not been detected in model hydrolytic studies of N^1-alkyl-purine heterocycles. There are also no apparent regions of amino acid sequence homologies between these two classes of purine hydrolases, and the mechanistic comparisons and contrasts should be a subject of future interest.

ACKNOWLEDGMENT

We are grateful to Prof. John N. Reeve for the gift of the pET-921 plasmid with the *M. vannielii hisI* gene. We thank John W. Burgner, II, for help in acquisition and analysis of the analytical ultra data and critical reading of an early form of the manuscript. We also thank Becky Auxier at the Chemical Analysis Laboratory (University of Georgia) and Peter Kane and Natalie Newlon at the Indiana State Chemist's Laboratory (Purdue University) for the ICP-ES and AAS analyses, respectively.

REFERENCES

1. Fani, R., Pietro, L., and Lazcano, A. (1995) *J. Mol. Evol. 41*, 760−774.
2. Winkler, M. E. (1996) in *Escherichia coli and Salmonella*, pp 485−505, American Society for Microbiology, Washington, DC.
3. Nar, H., Huber, R., Auerbach, G., Fischer, M., Hosl, C., Ritz, H., Bracher, A., Meining, W., Eberhardt, S., and Bacher, A. (1995) *Proc. Natl. Acad. Sci. U.S.A. 92*, 12120−12125.
4. Young, D. W. (1986) *Nat. Prod. Rep. 3*, 395−419.
5. Smith, D. W. E., and Ames, B. N. (1965) *J. Biol. Chem. 240*, 3056−3063.
6. Beckler, G. S., and Reeve, J. N. (1986) *Mol. Gen. Genet. 204*, 133−140.
7. Arndt, K. T., Styles, C., and Fink, G. R. (1987) *Science 237*, 874−880.
8. Oriol, E., Mendazalvarz, S., Barbe, J., and Gilbert, I. (1996) *Microbiology 142*, 2071−2078.
9. Xiang, S., Short, S. A., Wolfenden, R., and Carter, C. W., Jr. (1995) *Biochemistry 34*, 4516−4523.
10. Jones, W., Kurz, L. C., and Wolfenden, R. (1989) *Biochemistry 28*, 1242−1247.
11. Ausubel, F. M., Brent, R., Kingston, R. E., Moore, D. D., Seidman, J. G., Smith, J. A., and Struhl, K. (1994) *Current Protocols in Molecular Biology*, Greene Publishing and Wiley-Interscience, New York.
12. Sambrook, J., Fritsch, E. F., and Maniatis, T. (1989) *Molecular Cloning: A Laboratory Manual*, Cold Spring Harbor Laboratory Press, Cold Spring Harbor, NY.
13. Bradford, M. (1976) *Anal. Biochem. 72*, 248−254.
14. Schagger, H., and von Jagow, G. (1987) *Anal. Biochem. 166*, 368−379.
15. Garrrick-Silversmith, L., and Hartman, P. E. (1970) *Genetics 66*, 231−244.
16. Davisson, V. J., Deras, I. L., Hamilton, S. E., and Moore, L. L. (1994) *J. Org. Chem. 59*, 137−143.
17. Stallwagen, E. (1990) *Methods Enzymol. 182*, 317−328.
18. Laue, T., Hayes, D., and Philo, J. (1997) *Sedimentaion Interpretation Program*, version 1.0, University of New Hampshire, Durham, NH.
19. Milton, A. P. (1995) *Sedeq: A Suite of Programs for Analysis of Sedimentation Equilibrium*, version 4.0, National Institutes of Health, Bethesda, MD.
20. Auld, D. S. (1988) *Methods Enzymol. 158*, 13−14.
21. Auld, D. S. (1988) *Methods Enzymol. 158*, 110−117.
22. Beavis, R. C., and Chait, B. T. (1996) *Methods Enzymol. 270*, 519−551.
23. Han, J. C., and Han, G. Y. (1994) *Anal. Biochem. 220*, 5−10.
24. Bers, D., Patton, C., and Nuccitelli, R. (1994) in *Methods in Cell Biology*, Academic Press, New York.
25. Jaffe, E. K. (1993) *Comments Inorg. Chem. 15*, 67−92.
26. Vallee, B. L., and Auld, D. S. (1993) *Acc. Chem. Res. 26*, 543−551.
27. Berg, J. M., and Shi, Y. (1996) *Science 271*, 1081−1085.
28. Georgiou, G. (1996) in *Protein Engineering: Principals and Practice*, pp 101−127, Wiley Liss, New York.
29. Wei, C.-H., Chou, W.-Y., Ming, S.-H., Lin, S.-H., and Chang, G.-G. (1994) *Biochemistry 33*, 7931−7936.
30. Hlavaty, J. J., and Nowak, T. (1997) *Biochemistry 36*, 15514−15525.
31. Porter, J. A., Young, K. E., and Beachy, P. A. (1996) *Science 274*, 255−259.
32. Chong, S., Shao, Y., Paulus, H., Benner, J., Perler, F. B., and Xu, M.-Q. (1996) *J. Biol. Chem. 271*, 22159−22168.
33. Martin, R. G., Berberich, M. A., Ames, B. N., Davis, W. W., Goldberger, R. F., and Yourno, J. D. (1971) *Methods Enzymol. 27b*, 3−44.
34. O'Sullivan, W. J., and Smithers, G. W. (1979) *Methods Enzymol. 63*, 294−336.
35. Whitehouse, D. B., Tomkins, J., Lovegrove, J. U., Hopkinson, D. A., and McMillan, W. O. (1998) *Mol. Biol. Evol. 15*, 456−462.
36. Bork, P., and Koonin, E. V. (1994) *Proteins: Struct., Funct., Genet. 20*, 347−355.
37. Saraste, M., Sibbald, P. R., and Wittinghofer, A. (1990) *Trends Biochem. Sci. 179*, 430−434.
38. LoGrasso, P. V., Tu, C., Chen, X., Taoka, S., Laipis, P. J., and Silverman, D. N. (1993) *Biochemistry 32*, 5786−5791.

39. Bounaga, S., Laws, A. P., Galleni, M., and Page, M. I. (1998) *Biochem. J. 331*, 703−711.
40. Rawlings, N. D., and Barrett, A. J. (1995) *Methods Enzymol. 248*, 183−228.
41. Merkler, D. J., and Schramm, V. L. (1993) *Biochemistry 32*, 5792−5799.

BI982475X